Catalytic Wet Peroxide Oxidation of Phenol in a New Two-Impinging-Jets Reactor

ARTICLE *in* INDUSTRIAL & ENGINEERING CHEMISTRY RESEARCH · NOVEMBER 2009

Impact Factor: 2.59 · DOI: 10.1021/ie9004496

Catalytic Wet Peroxide Oxidation of Phenol in a New Two-Impinging-Jets Reactor

Asghar Molaei Dehkordi* and Amir Ali Ebrahimi

Department of Chemical and Petroleum Engineering, Sharif University of Technology, P. O. Box 11155-9465, Tehran, Iran

The catalytic wet peroxide oxidation (CWPO) of phenol with activated carbon (AC) as the catalyst has been successfully tested in a novel type of two-impinging-jets reactor (TIJR). The TIJR is characterized by a high-intensity reaction chamber, which is separated by a perforated plate from other parts of the reactor. The perforated plate was used as a filter to keep the catalyst particles within the reaction chamber. The influences of various operating and design parameters such as jet Reynolds number, feed flow rate, internozzle distance, and the jet diameter on the performance capability of the TIJR were investigated. As a result of the impinging process, turbulence, complex trajectory of AC particles, relatively high local concentration of hydrogen peroxide, and the relatively high local catalyst loading within the reaction chamber, the fractional disappearance of phenol and the total organic carbon (TOC) removal, obtained in the TIJR, increased compared to those obtained by conventional reaction systems such as packed-bed reactors and batch stirred-tank reactors. This may be attributed to the elimination of the external mass-transfer resistance around the solid particles, complex flow pattern within the reaction chamber, energy released as the result of impinging-jets collision, efficient use of hydrogen peroxide caused by the contact pattern provided by the TIJR, and the high-intensity mixing especially at the impingement zone of the TIJR.

1. Introduction

Phenol and substituted phenols are toxic pollutants commonly present in industrial waste effluent streams, particularly in wastewaters generated by oil refineries, coal conversion plants, petrochemical plants, polymeric resins, coal tar distillation, and pharmaceuticals, etc. Such wastewaters have become a major social and economic problem, as modern health-quality standards and environmental regulations have gradually become more restrictive. In addition, phenol and substituted phenols are used as raw materials in many petrochemical, chemical, and pharmaceutical industries.

Many methods including adsorption, biological degradation, chemical oxidation, and solvent extraction have been used to remove these compounds from water. Among these methods, adsorption is the most commonly applied process and it is effective for low to medium concentrations of phenolic compounds. A large number of theoretical and experimental results have been published using different adsorbents such as activated carbons, polymeric resins, and organoclays.[1−10] Activated carbon (AC) is the most commonly used adsorbent, which has been used in the adsorption and oxidation processes of phenol. Prior to recycling and material recovery from process or effluent waste streams, it is often necessary to separate and concentrate the useful or toxic compounds. Adsorption processes are able to concentrate solutes, especially in the case that these solutes are valuable and can be recycled.

One more promising processes for the treatment of phenolic wastewaters is catalytic wet peroxide oxidation (CWPO), which uses hydrogen peroxide as the oxidative agent. The CWPO process destroys a variety of organics released in wastewater effluents with the use of a catalyst, achieving a high conversion of the organic pollutants. Hence, the biological methods could serve as a complementary application for CWPO process. The latter process is carried out in a liquid phase and under mild operating conditions.[11−20]

The impinging-jets (IJ) technique is a unique flow configuration. The first patent for this technique was published by Bower.[21] The IJ technique was used by Elperin[22] for gas−solid suspensions and further developed by Tamir[23] in various chemical engineering processes. The IJ technique has been successfully applied to various chemical processes such as desorption,[24] absorption,[25−28] solid−liquid enzyme reactions,[29] copper extraction and stripping,[30,31] liquid−liquid reactions,[32,33] precipitation,[34,35] and crystallization with a calcium oxalate model system.[36]

The major goal of the present work was to test the performance capability of a new type of two-impinging-jets reactor for the CWPO of aqueous phenol.

2. Experimental Section

2.1. Chemicals and Adsorbent (or Catalyst). All chemicals used in this investigation including phenol, hydrogen peroxide, and manganese dioxide were of analytical grade supplied by Merck Co. Degassed and distilled water with conductivity ≤ 3 μS/cm was used in all the experiments. Commercial activated carbon (AquaSorb 101) was purchased from Jacobi Co. The specifications of activated carbon (AC) used in the present work are as follows: iodine number, 900 mg/g; surface area, 950 m^2/g; methylene blue, 200 mg/g; total pore volume, 0.88 cm^3/g; apparent density, 490 kg/m^3; wettability, 98%; pH, 8; mesh size range, 8−16 (mean diameter, 2.5 mm).

2.2. Methods of Analysis. The concentration of phenol was analyzed by high-performance liquid chromatography (HPLC, Waters, refractive index detector 2410). The Nova-Pak C18 column was used with a mixture of acetonitrile and distilled water (HPLC grade) with a ratio of 70/30 (w/w) as the mobile phase. The volumetric flow rate of the mobile phase was set to be 1.0 mL min^{-1}. The UV detector at the wavelength of 270 nm was used. The total organic carbon (TOC) was detected by

* To whom correspndence should be addressed. Tel.: +98-21-66165412. Fax: +98-21- 66022853. E-mail: amolaeid@sharif.edu.

10.1021/ie9004496 CCC: $40.75
Published on Web 09/25/2009

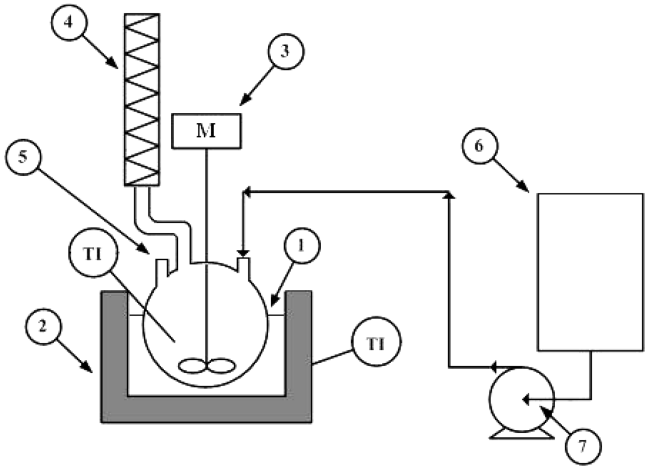

Figure 1. Experimental setup of BSTR: (1) Pyrex glass reactor; (2) thermostatic bath; (3) mixer; (4) reflux condenser; (5) sampling connection; (6) stainless steel H_2O_2 vessel; (7) H_2O_2 dosing pump.

a TOC analyzer (Skalar CA10). The concentration of hydrogen peroxide was determined by volumetric titration with Na_2SO_3 standard solution and excess amount of KI in an acidic medium.

2.3. Experimental Setup and Procedures. 2.3.1. Batch Stirred-Tank Reactor. Batch experiments were carried out in an 1 L Pyrex glass reactor. A schematic diagram of the batch stirred-tank reactor (BSTR) used in the present investigation is given in Figure 1. Phenol degradation experiments were carried out with 500 mL of aqueous phenol solution and an initial phenol concentration of 1.0 g/L. The reactor was placed in a thermostatted water bath with stirring to adjust the temperature of the solution within ±1 °C. The initial phenol solution was set to be in the range of pH = 5.5−5.8. When the desired solution temperature was reached, the preset amount of AC was added to the reactor, while hydrogen peroxide was continuously fed to the reactor. This point was taken as the "zero time" for the experimental records. The addition rate of hydrogen peroxide was set at a constant flow rate of 1.3 mM/min (i.e., 7.6 mL/(114 min) per 500 mL of phenol solution). This amount of H_2O_2 is almost equal to the stoichiometric amount required for the complete degradation of phenol. This low addition rate of hydrogen peroxide was chosen to minimize its consumption and to maximize its efficient use. During the course of the reaction, liquid samples were taken from the rector at preset time intervals with a syringe. An appropriate amount of MnO_2 was then immediately added to each sample in order to cease the progress of the reaction within the sampling bottles. The same procedure without hydrogen peroxide addition was used for the adsorption experiments, while the operating temperature and the initial phenol concentration could be varied according to Table 1.

2.3.2. Packed-Bed Reactor. The flow diagram of the experimental setup, shown in Figure 2, consisted of the following parts: packed-bed reactor (PBR) (1) equipped with a hot water jacket (2), where the diameter of the PBR was 2 cm and the working heights were 42 and 21 cm depending on the amount of AC used (i.e., corresponding to 8 and 4 g AC/L); H_2O_2 dosing pump made of stainless steel (SS) (3); hydrogen peroxide vessel made of SS (4); rotameter (5); aqueous phenol feed pump made of SS with a capacity of 40 L/min (6); aqueous feed vessel made of SS (7) equipped with a hot water jacket (8); sampling valve (9).

The phenol solution was prepared by dissolving the required amount of analytical-grade phenol in distilled water. All the experiments were performed with 6 L of aqueous phenol solution. The temperature of the feed solution was adjusted by means of hot water entering the jacket and the total circulation of the entire content of the feed vessel by means of the feed pump. In each experimental run, the phenol solution and the oxidative solution (i.e., H_2O_2) were continuously fed to the top of the PBR at given volumetric flow rates. The addition rate of H_2O_2 per unit volume of the solution was the same as that used in the BSTR (i.e., 91.2 mL/(112 min) per 6 L of phenol solution = 1.3 mM/min). The flow rate of the phenol solution was regulated using the rotameter. A recycled stream from the discharge of the feed pump was used to homogenize the entire content of the feed vessel. It should be added that preliminary measurements of the concentration of phenol solution within the feed vessel and that exiting the rotameter showed that such a setup results in the uniform concentration of phenol within the feed vessel. The effluent of PBR was recycled to the feed vessel. The samples were taken through the sampling connection of the feed vessel for the measurements. Analysis of the samples was performed by the aforementioned analytical methods for phenol concentration, hydrogen peroxide, and TOC. To cease the progress of the reaction within the sampling bottles, an appropriate amount of MnO_2 was immediately added to each sample.

For each data point, the experimental run was repeated at least two times, and thus each data point was determined on the basis of the mean value of at least two measurements of effluent concentration with a standard deviation of 1−3%. The same procedure without hydrogen peroxide addition was used for the adsorption experiments, while the operating temperature and the initial phenol concentration could be varied.

2.3.3. Two-Impinging-Jets Reactor. The flow diagram of the experimental setup, shown in Figure 3, consisted of the following parts: two-impinging-jets reactor (TIJR) whose dimensions were specified in Figure 3 (1); reaction chamber (2) equipped with two identical nozzles; perforated plate in order to keep the catalyst particles within the reaction chamber and to prevent the catalyst particles from exiting the reaction chamber (3); H_2O_2 feed vessel (4) made of SS; H_2O_2 dosing pump (5); rotameter (6) to regulate the feed solution flow rate; feed pump with a capacity of 40 L min^{-1} (7); feed vessel (8) equipped with a hot or cold water jacket (9); sampling connection (10).

The solution preparation procedure is the same as that stated in the PBR studies. In each experimental run, a given amount of AC was introduced into the reaction chamber. Then, the phenol solution and the oxidative solution (H_2O_2) were continuously fed to the reaction chamber through two identical jets located at the middle of reaction chamber at given volumetric flow rates. Note that the hydrogen peroxide was mixed with the recycled solution just at the entering point to the reaction chamber. The liquid jets exiting the opposed nozzles collide with each other in the middle part of reaction chamber and fluidize the AC particles, and after being passed through a filter to separate, the entrained AC particles were recycled to the feed vessel. The samples were taken through the sampling connection for the measurement. Analysis of the samples was performed according to the aforementioned procedure.

Note that the main aim of the upper part of reactor system was to prevent the circulation of entrained AC particles exiting the reaction chamber. Furthermore, the agitation promoted by the impinging jets is less aggressive than that obtained with conventional stirrers. In addition to the advantage of using the impinging-jets technique, the TIJR has the advantage of possessing one extra operating variable that is the position of the filter. This extra operating variable was not investigated in the present work. Note that the filter position may be used to

Table 1. Operating Conditions of the Batch Stirred-Tank Reactor (BSTR), Packed-Bed Reactor (PBR), and the Two-Impinging-Jets Reactor (TIJR)

mode of operation	adsorbent or catalyst loading (g/L)	initial phenol concn (g/L)	H_2O_2 addition rate (mM/min)	temp (°C)	volumetric flow rate (L/min)	working height (cm)	jet diam (mm)	internozzle distance (cm)
				BSTR				
oxidation	4	1.0	1.3	70				
adsorption	8	0.5	−	25				
				PBR				
oxidation	4	1.0	1.3	70	3.8	21		
adsorption	8	0.5	−	25	3.8	42		
				TIJR				
oxidation	4	1.0	1.3	70	3.8		2	1
oxidation	4	1.0	1.3	70	3.8		3	1
oxidation	4	1.0	1.3	70	3.8		4	1
oxidation	4	1.0	1.3	70	5		3	1
oxidation	4	1.0	1.3	70	6.5		3	1
oxidation	4	1.0	1.3	70	3.8		2	0.5
oxidation	4	1.0	1.3	70	3.8		2	2
oxidation	4	1.0	1.3	70	3.8		2	3
oxidation	4	1.0	1.3	70	3.8		2	4
oxidation	4	1.0	1.3	70	2		3	1
adsorption	4	0.5	−	25	5		3	1
adsorption	4	0.5	−	25	3.8		3	1
adsorption	4	0.5	−	25	6.5		3	1
adsorption	4	0.5	−	25	3.8		2	1
adsorption	4	0.5	−	25	3.8		4	1
adsorption	8	0.5	−	25	3.8		2	1
adsorption	4	1.0	−	70	3.8		2	1

enhance the contact time between the AC particles and feed solution because the reaction chamber can play the role of a fluidized-bed reactor as well.

It should be mentioned that each data point represents the mean value of at least two measurements of phenol concentration and the TOC with a standard deviation of 1−3%. The same procedure without hydrogen peroxide addition was used for the adsorption experiments, while the operating temperature and the initial concentration of phenol could be varied.

3. Results and Discussion

The operating conditions for the determination of phenol removal by adsorption, phenol disappearance by CWPO, and the TOC disappearance for the BSTR, PBR, and the TIJR are summarized in Table 1.

3.1. Definitions of Phenol Disappearance by CWPO, TOC Disappearance by CWPO, and the Phenol Removal by Adsorption. The phenol disappearance by CWPO process is normally defined as the fraction of phenol degraded and adsorbed through oxidation process. Use of the disappearance term instead of conversion is because the AC particles can play both the roles of the adsorbent and catalyst. Moreover, the phenol removal is normally defined as the fraction of phenol adsorbed by the adsorption process only. Furthermore, the TOC disappearance is defined as the amount of total organic carbon

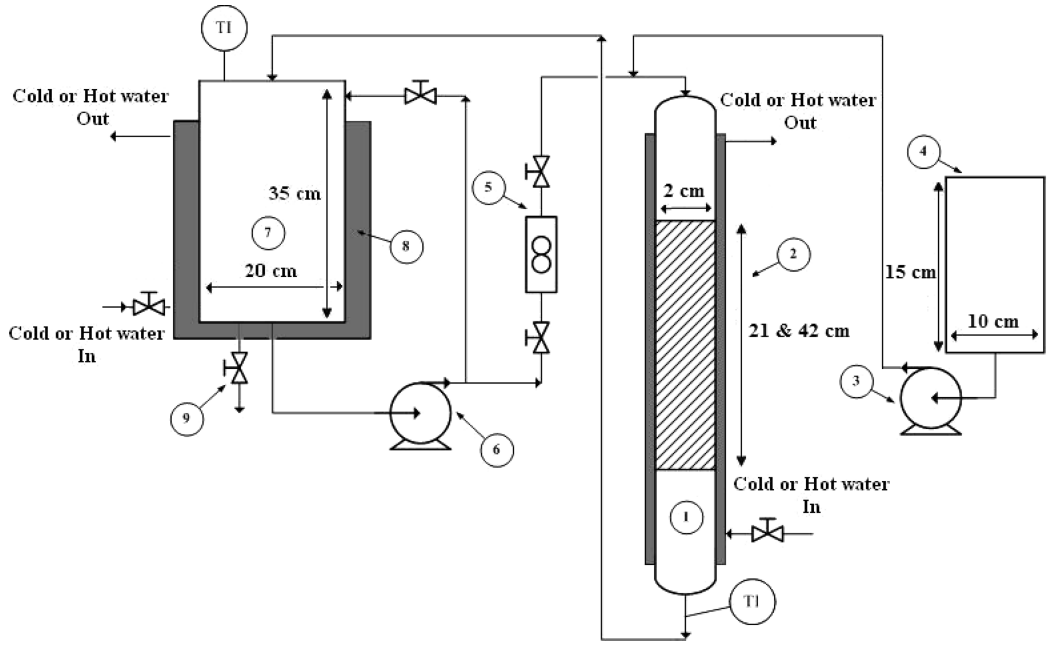

Figure 2. Experimental setup of PBR: (1) packed-bed reactor; (2) cold and hot water jacket; (3) H_2O_2 dosing pump; (4) stainless steel H_2O_2 vessel; (5) rotameter; (6) stainless steel feed pump; (7) stainless steel feed vessel; (8) cold and hot water jacket; (9) sampling valve.

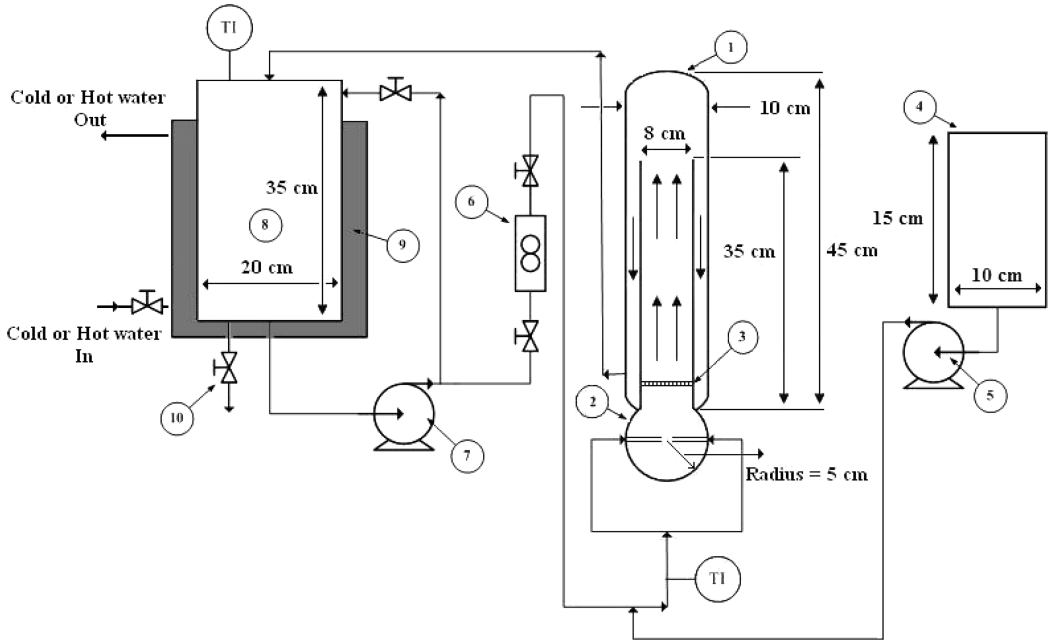

Figure 3. Experimental setup of the TIJR: (1) two-impinging-jets reactor; (2) mixing zone; (3) filter; (4) stainless steel H_2O_2 vessel; (5) H_2O_2 dosing pump; (6) rotameter; (7) stainless steel feed pump; (8) stainless steel feed vessel; (9) cold and hot water jacket; (10) sampling valve.

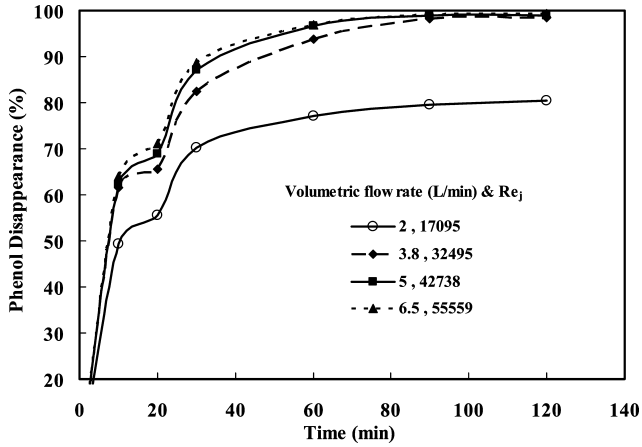

Figure 4. Effect of the volumetric flow rate and Re_j on the oxidation performance of the TIJR. Experimental conditions: Jet diameter = 3 mm; initial phenol concentration = 1 g/L; catalyst loading = 4 g/L; pH = 5.5; T = 70 °C.

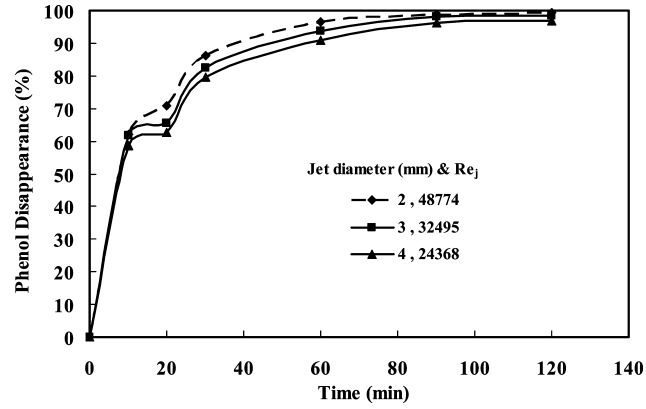

Figure 5. Effect of jet diameter and Re_j on the oxidation performance of the TIJR. Experimental conditions: Feed flow rate = 3.8 L/min; initial phenol concentration = 1.0 g/L; catalyst loading = 4.0 g/L; pH = 5.5; T = 70 °C.

decreased by the oxidation process, which is used as a measure of the progress of the phenol degradation in CWPO.

3.2. Oxidation Studies. 3.2.1. Effect of Volumetric Flow Rate of Feed Solution. Figure 4 shows the variations of the phenol disappearance vs time with the volumetric flow rate of the feed solution as a parameter at a jet diameter of 3 mm, initial phenol concentration of 1 g/L, and a catalyst loading of 4 g/L. As can be observed from this figure, an increase in the jet Reynolds number (Re_j) increases slightly the phenol degradation at a given time. Moreover, for the Re_j values greater than Re_j = 17095, the phenol disappearance increases significantly, because at this low-Re_j value the catalyst particles cannot be suspended within the reaction chamber. Note that the jet velocity exiting from the tip of the nozzles was calculated to be 2.36, 4.48, 5.9, and 7.67 m/s for the feed flow rates of 2, 3.8, 5, and 6.5 L/min, respectively.

3.2.2. Effect of Jet Diameter. To explore the effect of the jet diameter on the phenol disappearance, a number of experiments were carried out with the jet diameters ranging from 2 to 4 mm and at a constant volumetric flow rate of feed solution equal to 3.8 L/min, catalyst loading of 4.0 g/L, and an initial phenol concentration of 1.0 g/L. These experimental results are shown in Figure 5. A decrease in the jet diameter from 4 to 2 mm increases the jet Reynolds number from 24368 to 48774, consequently slightly increasing the phenol disappearance. The latter is due to much higher jet velocities and shear forces acting on the AC particles, as well as an increase in the bulk turbulence produced by eddies in the reaction chamber.

Figure 6 shows the variations of phenol disappearance with time as a function of jet Reynolds number (Re_j) obtained at different volumetric flow rates and jet diameters. As can be observed from this figure, the phenol disappearance obtained at Re_j of 42738, 48774, and 55559 are almost the same; therefore, it could be concluded that for the Re_j values greater than 42738, the phenol disappearance does not increases significantly. Furthermore, the experimental results for the Re_j = 1709 are not shown in this figure, because the catalyst particles cannot be suspended within the reaction chamber and, hence, the phenol disappearance was very low.

3.2.3. Effect of Internozzle Distance. To examine the influence of the internozzle distance on the performance capability of the TIJR, a number of oxidation experiments at a constant volumetric flow rate of 3.8 L/min, catalyst loading of

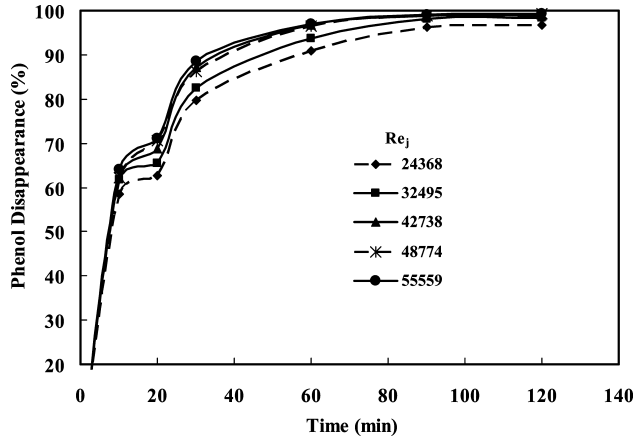

Figure 6. Effect of jet Reynolds number (Re_j) on the oxidation performance of the TIJR. Experimental conditions: Initial phenol concentration = 1.0 g/L; catalyst loading = 4.0 g/L; pH = 5.5; T = 70 °C.

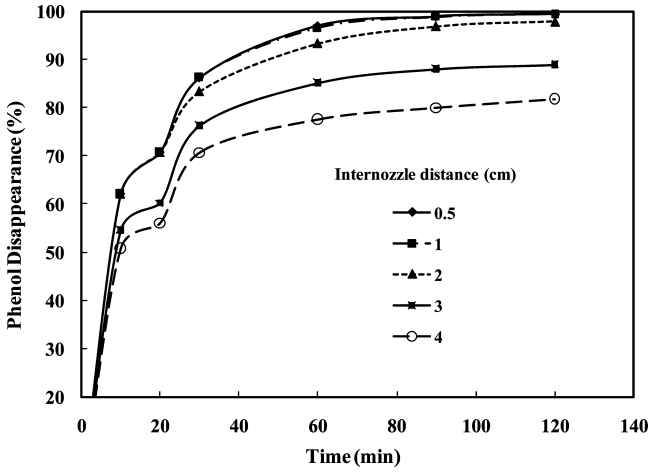

Figure 7. Phenol disappearance vs time for different internozzle distances. Experimental conditions: Flow rate = 3.8 L/min; initial phenol concentration = 1.0 g/L; catalyst loading = 4.0 g/L; jet diameter = 2.0 mm; pH = 5.5; T = 70 °C; H_2O_2 addition rate = 1.3 mM/min.

4.0 g/L, initial phenol concentration of 1.0 g/L, and the jet diameter of 2 mm with different internozzle distances ranging from 0.5 to 4 cm were carried out. These experimental results are shown in Figure 7. As can be observed from this figure, the phenol disappearances obtained at internozzle distances 0.5 and 1 cm are almost the same and further increasing the internozzle distance up to 2 cm slightly decreases the phenol disappearance due to a decrease in the turbulence of the reaction chamber. It should be also added that the turbulence obtained at internozzle distances greater than 2 cm were not be able to suspend completely the catalyst particles within the reaction chamber, so the phenol disappearance decreases profoundly.

3.2.4. Evaluation of Oxidation Performance Capability of the TIJR. To compare the performance capability of the TIJR in oxidation of phenol with that of other reactor types such as BSTR and PBR, a number of experiments with the identical catalyst loading, initial phenol concentration, oxidative solution flow rate per unit volume of phenol solution, circulating feed flow rate, and the operating temperature were carried out. According to these experiments, the performance capability of the TIJR compared with that of the conventional BSTR and PBR is evaluated on the basis of Figures 8 and 9, which represent the experimental data for the fractional disappearance of phenol as well as the TOC disappearance vs time for the CWPO process. On the basis of these experimental results, it can be concluded that the TIJR is superior to conventional

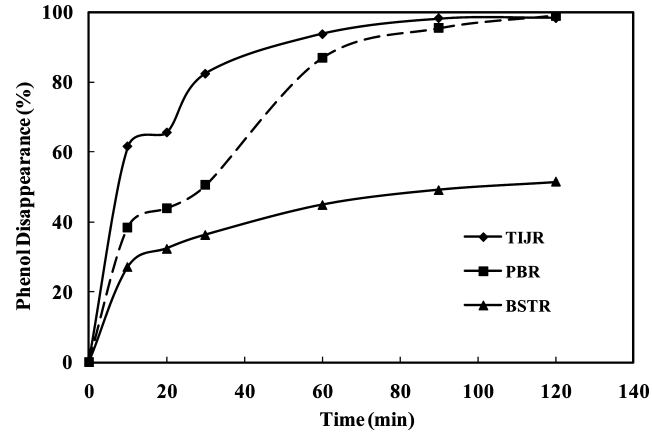

Figure 8. Phenol disappearance vs time for different types of reactor. Experimental conditions: Flow rate = 3.8 L/min; initial phenol concentration = 1.0 g/L; catalyst loading = 4.0 g/L; jet diameter = 2.0 mm; pH = 5.5; T = 70 °C; H_2O_2 addition rate = 1.3 mM/min.

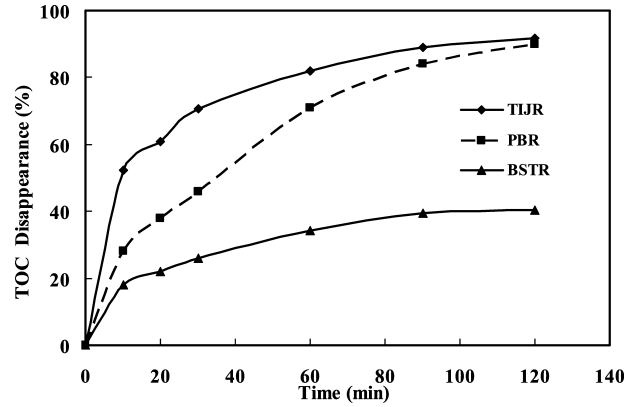

Figure 9. TOC disappearance vs time for different types of reactor. Experimental conditions: Flow rate = 3.8 L/min; initial phenol concentration = 1.0 g/L; catalyst loading = 4.0 g/L; jet diameter = 2.0 mm; pH = 5.5; T = 70 °C; H_2O_2 addition rate = 1.3 mM/min.

reactors. The following explanations can be given for such high fractional disappearance of phenol and the TOC disappearance obtained in the TIJR:

(1) Due to the complex flow pattern, strong collision of the jets, higher shearing forces acting on the AC particles, and high velocity of the AC particles within the reaction chamber especially at the impingement zone, the external mass-transfer resistance surrounding the solid AC particles (interphase mass-transfer resistances) could be eliminated.

(2) The oxidative solution (H_2O_2) was introduced to the top of the PBR, and thus there was a concentration gradient of H_2O_2 along the length of the PBR; consequently, the fractional disappearance of phenol could be lower than that of the TIJR, particularly at the times lower than 40 min. However, there is no such concentration gradient within the TIJR and all the catalyst particles contact with the uniform concentration of oxidative solution in the reaction chamber at any time.

(3) One more explanation for the much lower performance of the BSTR relative to the TIJR and PBR is that H_2O_2 solution spends a lot of time within the reaction system, where H_2O_2 could be decomposed by means of AC particles.[13,16] Moreover, the decomposition of H_2O_2 proceeds majorly through O_2 formation instead of OH radicals formation in the case of AC as the catalyst, which is a major drawback of using AC as the catalyst.[16] Therefore, the adsorption process becomes dominant, and the asymptotes shown in Figures 8 and 9 may be attributed to the saturation of the adsorbent cites as a result of the

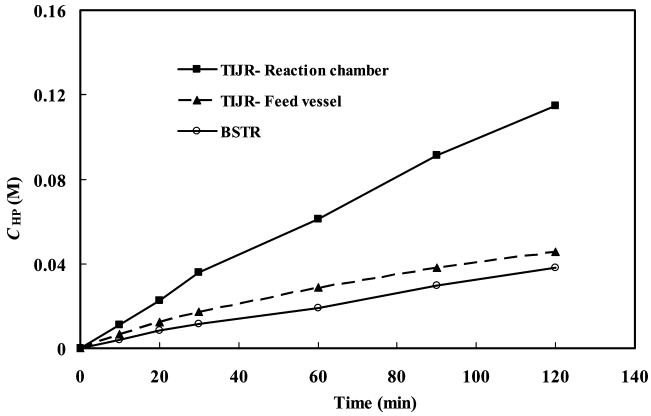

Figure 10. Comparison of local hydrogen peroxide concentration (C_{HP}) in the BSTR and TIJR. Experimental conditions: Flow rate = 3.8 L/min; initial phenol concentration = 1 g/L;, catalyst loading = 4.0 g/L; jet diameter = 2.0 mm; pH = 5.5; T = 70 °C; H_2O_2 addition rate = 1.3 mM/min.

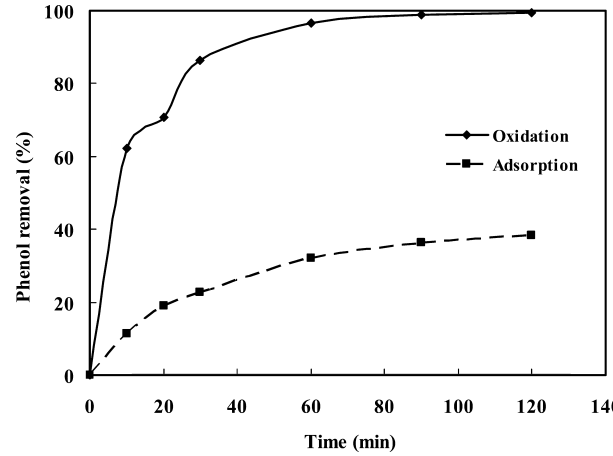

Figure 11. Comparison of phenol removal and disappearance obtained by adsorption and oxidation processes in the TIJR. Experimental conditions: Flow rate = 3.8 L/min; initial phenol concentration = 1.0 g/L; AC loading = 4.0 g/L; jet diameter = 2.0 mm; pH = 5.5; T = 70 °C; H_2O_2 addition rate = 1.3 mM/min.

adsorption process as well as the concentration of H_2O_2; consequently O_2 are not high enough to diffuse through the pores of AC particles and, hence, the reaction rate is low and the phenol disappearance does not increase with time. It should be added that similar trends have been reported by Zazo et al.[16] using AC as the catalyst in the BSTR. However, only a small fraction of oxidative solution contacts with the AC particles in the TIJR and PBR at any time, and much of the solution is in the feed vessel. Thus, the decomposition rate of H_2O_2 in the BSTR is much higher than that in the TIJR and the PBR; consequently, the fractional disappearance of phenol decreases.

(4) The local concentration of the oxidative solution within the reaction chamber of the TIJR is higher than that in the BSTR. To reach the same addition rate of H_2O_2 per unit volume of phenol solution (i.e., 1.3 mM/min) in the BSTR and TIJR with different volumes of solution within these reactors (i.e., BSTR, 500 mL; TIJR, 6000 mL), different volumetric flow rates of H_2O_2 (7.6 mL/(114 min) = 0.067 mL/min for BSTR and 91.2 mL/(112 min) = 0.814 mL/min for TIJR) were used. The above-mentioned H_2O_2 flow rate (i.e., 0.067 mL/min) was introduced to the reaction chamber of BSTR with the volume of 500 mL, whereas the higher H_2O_2 flow rate (0.814 mL/min) was introduced to the reaction chamber of TIJR with almost the same volume (i.e., the reaction chamber volume of TIJR is about 500 mL). This would result in the higher local concentration of hydrogen peroxide within the reaction chamber of TIJR, which is high enough to cause the high oxidant concentration gradient over the AC particle's cites. Therefore, the oxidant diffusion rate and consequently the reaction rate become high.

To verify this subject, the variations of concentration of oxidative solution within the reaction chamber of these reactors were detected and the obtained experimental results are presented in Figure 10. This efficient use of hydrogen peroxide in the TIJR is caused by the contact pattern provided by the TIJR that is described in the preceding items 3 and 4.

(5) Furthermore, the local catalyst loading in the reaction chamber of the TIJR is much higher than that in the BSTR (i.e., 24 g per 500 mL of reaction chamber of TIJR compared to 2 g per 500 mL of the reaction mixture in the BSTR). This high local catalyst loading as well as the relatively high local concentration of oxidant enhances the performance of TIJR relative to the BSTR.

Note that the hydrogen peroxide concentration in the feed vessel of TIJR given in Figure 10 clearly shows that, even at the end of the reaction, there is still an amount of hydrogen peroxide in the reaction mixture. Considering this fact that the stoichiometric amount of H_2O_2 was used in these experimental runs, it could be concluded that a fraction of phenol was removed by the adsorption process. To decrease the contribution of the adsorption process, all the oxidation experiments could be carried out at 70 °C.[16] To estimate the contribution of the adsorption process, one experiment under similar operating conditions in the absence of H_2O_2 solution was carried out. Figure 11 shows the comparison of phenol that disappeared by oxidation (i.e., CWPO) and adsorption processes in the TIJR. As can be observed from this figure, the phenol disappearance obtained by the oxidation process is about 61% higher than that obtained by the adsorption process.

Despite this fact that an unknown amount of phenol was removed by the adsorption process, the comparison of phenol and TOC disappearances obtained in TIJR and BSTR, which are illustrated in Figures 8 and 9 as well as the H_2O_2 concentration in the reaction chambers of TIJR and BSTR given in Figure 10, clearly show that the oxidation performance of TIJR in comparison with the conventional PBR and BSTR is promising.

(6) To calculate the power input requirements for both TIJR and PBR, a number of experiments were carried out to measure pressure drops. Note that the power input requirements for both TIJR and PBR are the sum of the power required for the feed and H_2O_2 pumps. To determine these power inputs, during the experiments, the pressure drops across the TIJR and PBR were measured. The total power input requirement (P_t) was determined as follows:

$$P_t = (Q_{PH} + Q_{HP})\Delta p_t \cong (Q_{PH})\Delta p_t$$

where Q_{PH}, Q_{HP}, and Δp_t are the volumetric flow rate of phenol solution, volumetric flow rate of H_2O_2 solution, and the total pressure drops across the reactors, respectively. Figure 12 shows the comparison of the power input requirements for two different reactors (i.e., TIJR and PBR). As can be observed from this figure, the power consumption for the TIJR is lower than that of PBR at the same volumetric flow rate (i.e., 13.7 W for PBR vs 2.5 W for TIJR at a volumetric flow rate of 3.8 L/min). Therefore, the higher oxidation performance with lower power consumption achieved by TIJR is promising. To explore whether the same oxidation performance could be achieved by lower volumetric flow rates and consequently lower power consumptions in the PBR or not, one experiment was carried out with

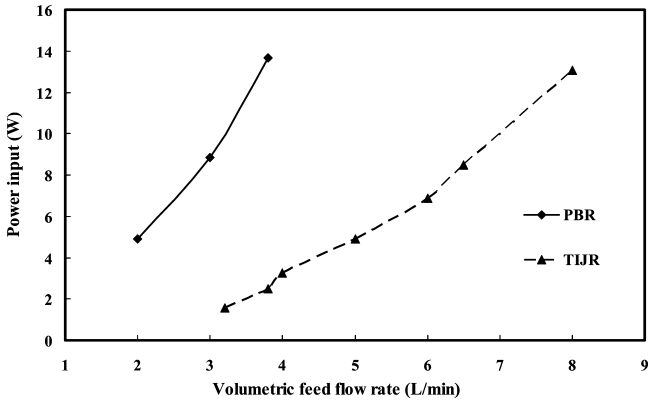

Figure 12. Power input requirements for the TIJR and PBR.

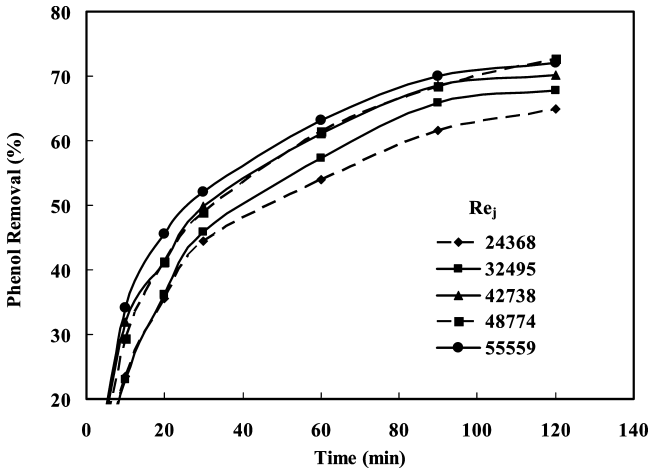

Figure 13. Effect of Re_j on the adsorption performance of TIJR. Experimental conditions: Initial phenol concentration = 0.5 g/L; adsorbent loading = 4.0 g/L; pH = 5.5; T = 25 °C.

the same operating conditions at a volumetric flow rate of 2 L/min. The experimental results were the same as those obtained at a flow rate of 3.8 L/min, so increasing the flow rate higher than 2 L/min does not increase the oxidation performance of PBR. Considering the power input requirement for the PBR at a volumetric flow rate of 2 L/min (i.e., 4.9 W), it could be concluded that even at this lower flow rate, the power consumption is higher than that of the TIJR at a flow rate of 3.8 L/min (i.e., 2.5 W). Hence, once again this result verifies the superiority of TIJR relative to the PBR.

3.3. Adsorption Studies. 3.3.1. Effect of Jet Reynolds Number. A number of experimental runs were carried out to investigate the effect of the Re_j on the phenol removal while other operating parameters were kept unchanged. Figure 13 illustrates the variations of the phenol removal vs time with the Re_j value as a parameter at the jet diameter = 3 mm, initial phenol concentration = 0.5 g/L, and the adsorbent loading = 4.0 g/L. As can be observed from this figure, an increase in the Re_j value leads to an increase in the phenol removal at the same operating time. Note that the jet velocities exiting from the tip of the nozzles and the corresponding Re_j values ($Re_j = (\rho u_j d_j)/(\mu)$) were calculated to be 4.48, 5.9, and 7.67 m/s and 32495, 42738, and 55559, respectively. The obtained results are the same as those observed in the oxidation process and similarly can be explained by an increase in the mixing and turbulence due to both the impinging process and high-rate shear forces acting on the AC particles.

3.3.2. Evaluation of Adsorption Performance Capability of the TIJR. To compare the adsorption capability of the TIJR compared with that of other contactor types, a number of

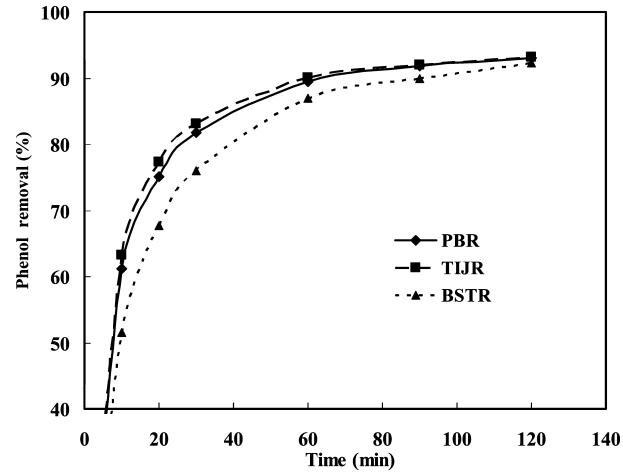

Figure 14. Phenol removal by adsorption vs time for different types of contactor. Experimental conditions: Flow rate = 3.8 L/min; initial phenol concentration = 0.5 g/L; jet diameter = 2.0 mm; adsorbent loading = 8.0 g/L; pH = 5.5; T = 25 °C.

adsorption experiments were carried out by using the BSTR and the PBR under the same operating conditions used in the TIJR. These experimental results are shown in Figure 14, which illustrates the adsorption data for various types of contactor vs time. It may be concluded that the performance capability of the TIJR and PBR with respect to the adsorption of phenol is slightly better than that of the BSTR. In addition, these experimental data once again verify the superiority of the TIJR for the phenol removal.

4. Conclusions

A novel type of the TIJR was proposed and tested as a chemical reactor for the CWPO of phenol solutions as a typical model system of wet oxidation treatment of effluent waste streams. Some aspects of the oxidation and adsorption behaviors of the TIJR were investigated within a range of operating conditions such as the jet Reynolds number and internozzle distance.

From the experimental results, it was observed that the fractional disappearance of phenol and the TOC disappearance obtained in the TIJR were much higher than those obtained in conventional reactors such as batch stirred-tank reactors and were higher than those obtained in a packed-bed reactor. This may be attributed to the elimination of the external mass-transfer resistance around the solid particles, complex flow pattern within the reaction chamber, energy released as the result of impinging-jets collision, efficient use of hydrogen peroxide as a result of the contact pattern provided by the TIJR, the high-intensity mixing especially at the impingement zone, relatively high local concentration of H_2O_2, and relatively high local catalyst loading within the reaction chamber.

Acknowledgment

The authors thank Mr. Iman Safari for his help and participation in the experimental work and gratefully acknowledge Sharif University of Technology (Tehran, Iran) for providing financial support.

Literature Cited

(1) Vazquez, G.; Alonso, R.; Freire, S.; Alvarez, J. G.; Antorrena, G. Uptake of phenol from aqueous solutions by adsorption in a Pinus pinaster bark packed bed. *J. Hazard. Mater.* **2006**, *B133*, 61–67.

(2) Aksu, Z.; Ferda, G. F. Biosorption of phenol by immobilized activated sludge in a continuous packed bed: Prediction of breakthrough curve. *Process Biochem.* **2004**, *39*, 599–613.

(3) Otero, M.; Zabkova, M.; Rodrigues, A. E. Phenolic wastewaters purification by thermal parametric pumping: modeling and pilot-scale experiments. *Water Res.* **2005**, *39*, 3467–3478.

(4) Gupta, V. K.; Srivastava, S. K.; Tyagi, R. Design parameters for the treatment of phenolic wastes by carbon columns (obtained from fertilizer waste material). *Water Res.* **2000**, *34*, 1543–1550.

(5) Bercic, G.; Pintar, A. Desorption of phenol from activated carbon by hot water regeneration. Desorption isotherms. *Ind. Eng. Chem. Res.* **1996**, *35*, 4619–4625.

(6) Garcia, A.; Silva, J.; Ferreira, L.; Leitao, A.; Rodrigues, A. Regeneration of fixed-bed adsorbers saturated with single and binary mixtures of phenol and m-cresol. *Ind. Eng. Chem. Res.* **2002**, *41*, 6165–6174.

(7) Cotoruelo, L. M.; Marques, M. D.; Rodriguez-Mirasol, J.; Cordero, T.; Rodriguez, J. J. Adsorption of aromatic compounds on activated carbons from ligin: Kinetic study. *Ind. Eng. Chem. Res.* **2007**, *46*, 2853–2860.

(8) Canizares, P.; Carmona, M.; Baraza, O.; Delgado, A.; Rodrigo, M. A. Adsorption equilibrium of phenol onto chemically modified activated carbon F400. *J. Hazard. Mater.* **2006**, *B131*, 243–248.

(9) Carmona, M.; De Luca, A.; Valverde, J. L.; Velasco, B.; Rodrıguez, J. F. Combined adsorption and ion exchange equilibrium of phenol on Amberlite IRA- 420. *Chem. Eng. J.* **2006**, *117*, 155–160.

(10) Podkoscienly, P.; Nieszporek, K.; Szabelski, P. Adsorption from aqueous phenol solutions on heterogeneous surfaces of activated carbons—Comparison of experimental data and simulations. *Colloids Surf., A* **2006**, *277*, 52–58.

(11) Catrinescu, C.; Teodosiu, C.; Macoveanu, M.; Miehe-Brendle, J.; Dred, R. L. Catalytic wet peroxide oxidation of phenol over Fe-exchanged pillared beidellite. *Water Res.* **2003**, *37*, 1154–1160.

(12) Guo, J.; Al-Dahhan, M. Catalytic wet oxidation of phenol by hydrogen peroxide over pillared clay catalyst. *Ind. Eng. Chem. Res.* **2003**, *42*, 2450–2460.

(13) Debellefontaine, H.; Chakchouk, M.; Foussard, J. N.; Tissot, D.; Striolo, P. Treatment of organic aqueous wastes: wet air oxidation and wet peroxide oxidation. *Environ. Pollut.* **1996**, *92*, 155–164.

(14) Valkaj, K. M.; Katovic, A.; Zrncevic, S. Investigation of the catalytic wet peroxide oxidation of phenol over different types of Cu/ZSM-5 catalyst. *J. Hazard. Mater.* **2007**, *144*, 663–667.

(15) Park, J. N.; Wang, J.; Choi, K. Y.; Dong, W. Y.; Hong, S. I.; Lee, C. W. Hydroxylation of phenol with H_2O_2 over Fe^{2+} and/or Co^{2+} ion-exchanged NaY catalyst in the fixed-bed flow reactor. *J. Mol. Catal. A: Chem.* **2006**, *247*, 73–79.

(16) Zazo, J. A.; Casas, J. A.; Mohedano, A. F.; Rodrıguez, J. J. Catalytic wet peroxide oxidation of phenol with a Fe/active carbon catalyst. *Appl. Catal., B* **2006**, *65*, 261–268.

(17) Carriazo, J.; Guelou, E.; Barrault, J.; Tatibouet, J. M.; Molina, R.; Moreno, S. Catalytic wet peroxide oxidation of phenol by pillared clays containing Al-Ce-Fe. *Water Res.* **2005**, *39*, 3891–3899.

(18) Zrncevic, S.; Gomzi, Z. CWPO: An environmental solution for pollutant removal from wastewater. *Ind. Eng. Chem. Res.* **2005**, *44*, 6110–6114.

(19) Carriazo, J. G.; Guelou, E.; Barrault, J.; Tatibouet, J. M.; Moreno, S. Catalytic wet peroxide oxidation of phenol over Al-Cu or Al-Fe modified clays. *Appl. Clay Sci.* **2003**, *22*, 303–308.

(20) Barrault, J.; Tatibouet, J. M.; Papayannakos, N. Catalytic wet peroxide oxidation of phenol over pillared clays containing iron or copper species. *Chemistry* **2000**, *3*, 777–783.

(21) Bower, H. Process of Facilitating Chemical Reactions. U.S. Patent No. 410067, 1889.

(22) Elperin, I. T. Heat and mass transfer in opposing currents (in Russian). *J. Eng. Phys.* **1961**, *6*, 62.

(23) Tamir, A. *Impinging streams reactors: Fundamentals and applications*; Elsevier: Amsterdam, The Netherlands, 1994.

(24) Herskowits, D.; Herskowits, V.; Tamir, A. Desorption of acetone in a two-impinging-streams spray desorber. *Chem. Eng. Sci.* **1987**, *42*, 2331.

(25) Tamir, A.; Herskowits, D.; Herskowits, V. Impinging-jets absorber. *Chem. Eng. Process.* **1990**, *28*, 165.

(26) Tamir, A.; Herskowits, D.; Herskowits, V.; Stephen, K. Two-impinging jets absorber. *Ind. Eng. Chem. Res.* **1990**, *29*, 272.

(27) Kleingeld, A. W.; Lorenzen, L.; Botes, F. G. The development and modeling of high-intensity impinging streams jet reactors for effective mass transfer in heterogeneous systems. *Chem. Eng. Sci.* **1999**, *54*, 4991.

(28) Herskowits, D.; Herskowits, V.; Stephen, K.; Tamir, A. Characterization of a two-phase impinging jet absorber: II. Absorption with chemical reaction of CO_2 in NaOH solutions. *Chem. Eng. Sci.* **1990**, *5*, 1281.

(29) Dehkordi, A. M. Novel type of two-impinging-jets reactor for solid-liquid enzyme reactions. *AIChE J.* **2006**, *52*, 692.

(30) Dehkordi, A. M. A novel two-impinging-jets reactor for copper extraction and stripping processes. *Chem. Eng. J.* **2002**, *87*, 227.

(31) Dehkordi, A. M. Experimental investigation of an air-operated two impinging-streams reactor for copper extraction processes. *Ind. Eng. Chem. Res.* **2002**, *41*, 2512.

(32) Dehkordi, A. M. Liquid-liquid extraction with chemical reaction in a novel impinging-jets reactor. *AIChE J.* **2002**, *48*, 2230.

(33) Dehkordi, A. M. Liquid−liquid extraction with an interphase chemical reaction in an air-driven-two-impinging-streams reactor: Effective interfacial area and overall mass-transfer coefficient. *Ind. Eng. Chem. Res.* **2002**, *41*, 4085.

(34) Johnson, B. K.; Prudhomme, R. K. Chemical processing and micromixing in confined impinging jets. *AIChE J.* **2003**, *49*, 2264.

(35) Mahajan, A. J.; Kirwan, D. J. Micromixing effect in a two-impinging-jets precipitator. *AIChE J.* **1996**, *42*, 1801.

(36) Hacherl, J. M.; Paul, E. L.; Buettner, H. M. Investigation of impinging-jet crystallization with a calcium oxalate model system. *AIChE J.* **2003**, *49*, 2352.

Received for review March 19, 2009
Revised manuscript received August 31, 2009
Accepted September 4, 2009

IE9004496